A Statistical Approach to Spark Advance Mapping

Enrico Corti[1]
e-mail: enrico.corti2@unibo.it

Claudio Forte
e-mail: claudio.forte@mail.ing.unibo.it

Department of Mechanical, Aerospace Nuclear Engineering and Metallurgy (DIEM),
University of Bologna,
Viale Risorgimento 2,
40136 Bologna, Italy

Engine performance and efficiency are largely influenced by combustion phasing. Operating conditions and control settings influence the combustion development over the crankshaft angle; the most effective control parameter used by electronic control units to optimize the combustion process for spark ignition engines is spark advance (SA). SA mapping is a time-consuming process, usually carried out with the engine running in steady state on the test bench, changing SA values while monitoring brake mean effective pressure, indicated mean effective pressure (IMEP), and brake specific fuel consumption (BSFC). Mean values of IMEP and BSFC for a test carried out with a given SA setting are considered as the parameters to optimize. However, the effect of SA on IMEP and BSFC is not deterministic, due to the cycle-to-cycle variation; the analysis of mean values requires many engine cycles to be significant of the performance obtained with the given control setting. Finally, other elements such as engine or components aging, and disturbances like air-to-fuel ratio or air, water, and oil temperature variations could affect the tests results; this facet can be very significant for racing engine testing. This paper presents a novel approach to SA mapping with the objective of improving the performance analysis robustness while reducing the test time. The methodology is based on the observation that, for a given running condition, IMEP can be considered a function of the combustion phasing, represented by the 50% mass fraction burned (MFB50) parameter. Due to cycle-to-cycle variation, many different MFB50 and IMEP values are obtained during a steady state test carried out with constant SA. While MFB50 and IMEP absolute values are influenced by disturbance factors, the relationship between them holds, and it can be synthesized by means of the angular coefficient of the tangent line to the MFB50-IMEP distribution. The angular coefficient variations as a function of SA can be used to feed a SA controller, able to maintain the optimal combustion phasing. Similarly, knock detection is approached by evaluating two indexes; the distribution of a typical knock-sensitive parameter (maximum amplitude of pressure oscillations) is related to that of CHR_{NET} (net cumulative heat release), determining a robust knock index. A knock limiter controller can then be added in order to restrict the SA range to safe values. The methodology can be implemented in real time combustion controllers; the algorithms have been applied offline to sampled data, showing the feasibility of fast and robust automatic mapping procedures. [DOI: 10.1115/1.4000294]

1 Introduction

Spark ignition (SI) engine performance are influenced by combustion phasing and duration. As it is shown in Refs. [1–5] the combustion process of a SI engine can be represented by means of phenomenological models such as Wiebe functions. A Wiebe function is defined by means of four parameters, as shown in the following equation:

$$x_b = 1 - e^{-a\cdot(\theta - \theta_{SOC}/\Delta\theta)^{m_w+1}} \quad (1)$$

The parameter a is related to the mass fraction burned at the end of the combustion process (i.e., when $\theta = \theta_{SOC} + \Delta\theta$), thus, it can be considered as a constant. It can also be shown [5] that m_W is related to the shape that the rate of heat release (ROHR) curve can assume for given values of θ_{SOC} and $\Delta\theta$. Basically, this means that m_W is related to the ROHR peak value.

The optimal combustion control setting should vary the three free parameters in order to achieve the best performance. Sometimes the control actions influence m_W, θ_{SOC}, and $\Delta\theta$ at the same time; in this case all the combustion characteristics can be synthesized with a single parameter. Typically, the MFB50 is used for this purpose since it catches the three main facets of the combustion event. SA can be considered as one of those control factors changing combustion phasing (θ_{SOC}), duration ($\Delta\theta$), and shape (m_W) at the same time; this allows describing SA effects, simply in terms of MFB50. The best SA setting is that maintaining the MFB50 near to the optimal value; this setting implicitly optimizes θ_{SOC}, $\Delta\theta$, and m_W. The optimization target is usually set in terms of maximum IMEP, but the process could involve other parameters such as BSFC, pollutants emission, noise, etc.

The SA mapping procedure is aimed at determining those SA values that the electronic control units (ECU) will use in open loop control during engine operation. The process is usually carried out on the test bench with a fixed SA level, keeping the engine in steady conditions for many engine cycles (sometimes many thousands) to filter out the effect of cycle-to-cycle variation. Data are usually collected for a given engine running condition with different SA values, and finally, the operations are repeated for each breakpoint defining the engine operating range. This means that SA sweeps must be performed for different engine speed, load, and sometimes, oil/water temperature, gasoline temperature, etc. The mapping operation is time consuming, and especially in racing applications, very expensive, due to the short engine life and the risk of exploring dangerous (knocking) running conditions during the sweep.

Patterson [6] defines a methodology to speed up the mapping procedure by using engine speed sweep instead of step test data. The technique makes use of the MFB50 parameter for combustion phasing, but it lacks of an insight on how the target value can be

[1]Corresponding author.

Contributed by the International Gas Turbine Institute of ASME for publication in the JOURNAL OF ENGINEERING FOR GAS TURBINES AND POWER. Manuscript received May 21, 2009; final manuscript revised May 23, 2009; published online May 27, 2010. Editor: Dilip R. Ballal.

selected. Haskara et al. [7] proposed the use of a new combustion invariant strictly related to the Wiebe function shape. The best phasing should be attained as the maximum acceleration of mass fraction burned (MAMFB) is placed at top dead center (TDC). However, the amount of calculations necessary to evaluate the invariant suggests using a different parameter for real time applications.

This paper aims to show how combustion information gathered by means of an in-cylinder pressure sensor can be used in order to shorten mapping time. The proposed mapping methodology determines the optimal control setting by means of two proportional-integer-derivative (PID) controllers regulating SA, based on indicated parameter information. The first one is targeted at the achievement of the optimal combustion phasing, and the second one at the detection of knock.

The two controllers share a characteristic. Their input (error) is defined to follow a target trend and not just a target value. The combustion phasing controller, for example, will not follow a given reference value for MFB50 or a target value for IMEP. The MFB50 and IMEP distributions are related, and a parameter intrinsically representing the actual position in the MFB50-IMEP curve can be defined. This parameter can be used as an input for the controller, guaranteeing the achievement of the maximum IMEP independently of how external disturbances (cycle-to-cycle variation, changes in air temperature, engine aging) affect IMEP absolute values. A slightly different approach is used for knock detection and control. In this case, the input error is defined based on the relationship between distributions of two different knock indexes.

A set of tests with different SA values can be substituted by a single test, where SA values are automatically changed by the controller, taking into account both performance and knock behavior. The SA sweep is carried out in real time by the controllers, whose output will finally converge to the best (maximum IMEP) possible (nonknocking) SA.

2 SA Effect on Combustion

To highlight the effect of SA on combustion development, tests have been carried out on the test bench in steady state conditions on a FIAT Fire 1.2 l four cylinders port fuel injection (PFI) gasoline engine. Engine speed was kept constant by means of the eddy-current brake controller; a brushless motor driving the throttle was feedback controlled, based on the intake manifold pressure to set engine load. Intake manifold pressure and temperature, air to fuel ratio (AFR), coolant, and oil temperatures have been maintained constant during the tests. Each test, counting 1000 engine cycles, has been executed holding a different SA value, up to and over audible knock. In-cylinder pressure was measured by means of Kistler 6117BCD15 measuring spark plugs and 5064B21 charge amplifiers. Angular position tracking has been carried out by means of a sensor instrument FIA-F optical sensor, coupled to a crankshaft-mounted measurement disk with 120 markers per revolution. The in-cylinder pressure signals have been sampled at 100 kHz, while the angular reference signal (encoder) has been detected by means of a timer-counter digital channel with a 20 MHz clock. All the signals have been sampled using a Wavebook 516 Data Acquisition System.

The in-cylinder pressure signals have been low-pass filtered by means of an antialiasing analog filter set at 30 kHz; the filter delay has been compensated in order to avoid referencing errors. A 3 kHz zero-delay low-pass fourth order Butterworth digital filter has been used for IMEP and net cumulative heat release (CHR_{NET}) calculations in order to eliminate the combustion chamber resonance effect. This allows isolating the mean combustion chamber conditions contribution to CHR and indicated work trends, while rejecting the components related to local pressure oscillations.

As already mentioned, the combustion process can be described by means of three parameters that can be reduced to 1 if the control action changes the combustion phasing, duration, and shape at the same time. Figure 1 shows that this hypothesis can be applied to SA control; the combustion phasing (MFB10), duration (MFB90-MFB10), and shape (represented by the maximum value of the ROHR curve) are all clearly related to MFB50.

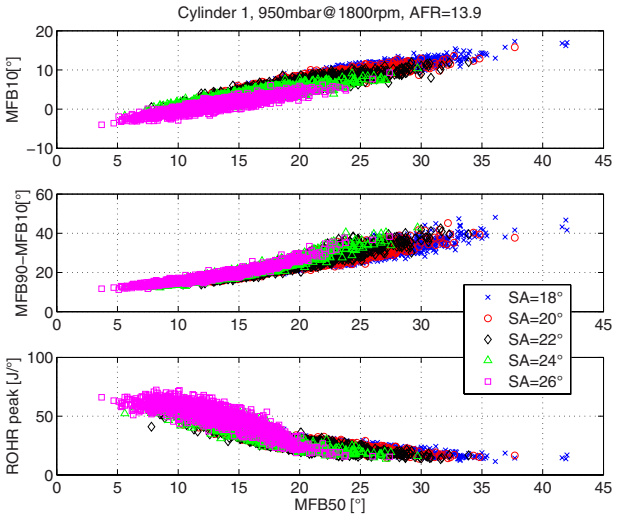

Fig. 1 Combustion phasing, duration, and shape as a function of MFB50

The SA value influences the combustion development over the crankshaft angle, but it is not a deterministic control parameter. Engine cycles carried out with the same value of SA may show very different combustion phasing. On the other side, the relationship between performance (IMEP) and combustion characteristics (MFB50) does not depend on the SA value; IMEP and MFB50 distributions achieved with different SA settings form a unique trace (Fig. 2). In other words, SA sets the IMEP and MFB50 values range, and ranges corresponding to different SA superimpose; what they have in common is that they are placed over the same IMEP-MFB50 curve.

Figure 2 shows how the distributions referring to different SA levels partially superimposed, forming the typical parabola curve. A possible way to optimize SA is to change its value according to the position that the points representing a given buffer of previous engine cycles assume in the plot. Obviously the objective will be to maintain the combustion phasing as near as possible to the maximum IMEP value. If the relation between the two distribu-

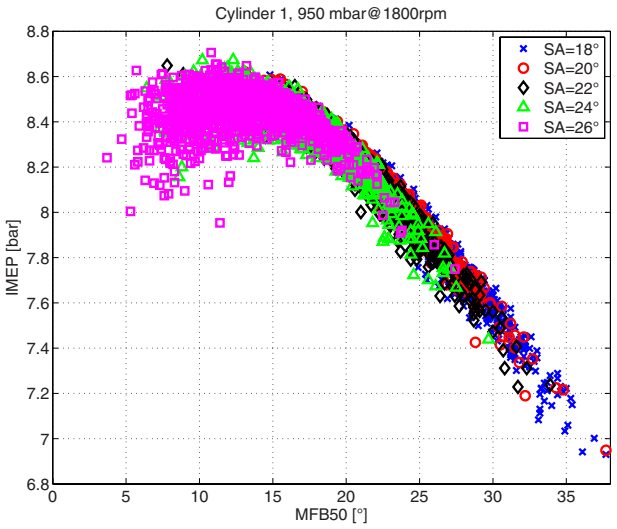

Fig. 2 Relationship between IMEP and MFB50 distributions

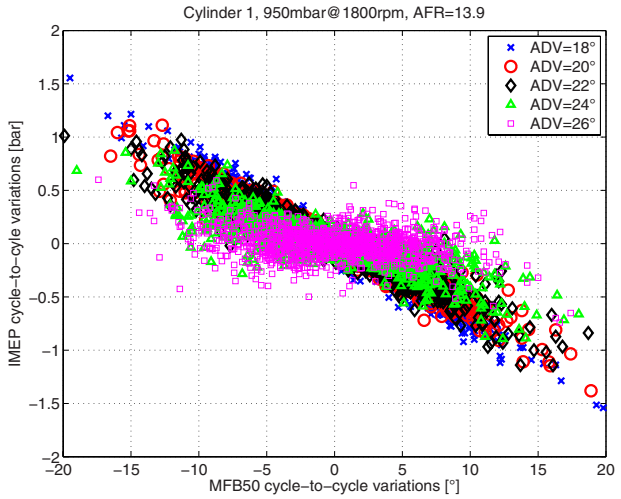

Fig. 3 IMEP versus MFB50 cycle-to-cycle variations

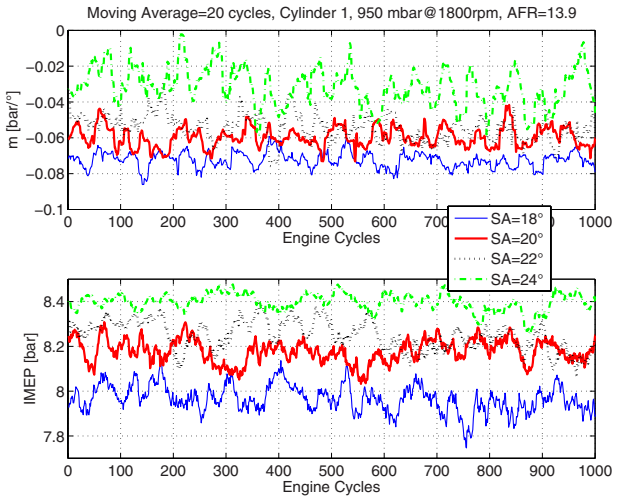

Fig. 4 *m* and IMEP evolution over the tests (moving average over 20 cycles)

tions is as clear as in Fig. 2, a low number of engine cycles is sufficient to draw the conclusion on the direction and amplitude of the SA variation necessary to reach the optimal condition. This operation can be done manually or by means of a controller; the combustion must be advanced if, within a buffer of engine cycles with the same SA, IMEP is higher for those cycles showing lower MFB50 values. The optimal SA setting is reached as the effect on IMEP of the engine cycles placed on the right of the parabola maximum is compensated by that of the cycles placed on the left.

The concept has to be expressed analytically for the controller, feeding it with an error input that will finally allow reaching the optimal SA. The maximum of the curve is, by definition, the point where the derivative is equal to zero; the derivative of IMEP with respect to MFB50 can perfectly play the role of the controller input (error). When the derivative is negative, the SA must be incremented, when it is positive SA must be reduced, and when it is equal to zero, the controller has to take no action since the combustion phasing is optimal.

Figure 3 shows the same information of Fig. 2, focusing the attention on how the curve derivative changes with SA; each point in the plot represents the cycle-to-cycle difference of IMEP versus that of MFB50. The n-th point reported in the plot is defined by coordinates (MFB50(n)-MFB50($n-1$); IMEP(n)-IMEP($n-1$)). The distributions rotate counter-clockwise as SA is increased, which means that the maximum of the parabola is being approached. The last distribution (SA=26 deg) is almost horizontal; in this case, the mean derivative tends to zero, i.e., the optimal combustion phasing has been reached.

In order to define a parameter representative of combustion characteristics related to the actual SA, the calculation of the derivative must take into account a given number of engine cycles. Equation (2) highlights the cycle-to-cycle variation terms for MFB50 and IMEP, while $\delta_{\text{MFB50}}|_i$ and $\delta_{\text{IMEP}}|_i$ refer to the differences between two subsequent cycles, and $\Delta_{\text{MFB50}}|_j$ and $\Delta_{\text{IMEP}}|_j$ are vectors collecting the $\delta_{\text{MFB50}}|_i$ and $\delta_{\text{IMEP}}|_i$ values for the last N cycles

$$\begin{aligned}
\delta_{\text{MFB50}}|_i &= \text{MFB50}|_i - \text{MFB50}|_{i-1} \\
\delta_{\text{IMEP}}|_i &= \text{IMEP}|_i - \text{IMEP}|_{i-1} \\
\Delta_{\text{MFB50}}|_j &= [\delta_{\text{MFB50}}|_{j-N+1} \cdots \cdot \delta_{\text{MFB50}}|_j] \\
\Delta_{\text{IMEP}}|_j &= [\delta_{\text{IMEP}}|_{j-N+1} \cdots \cdot \delta_{\text{IMEP}}|_j]
\end{aligned} \tag{2}$$

A linear interpolation $\Delta_{\text{IMEP}}|_j$ as a function of $\Delta_{\text{MFB50}}|_j$ allows defining the parameter $m|_j$ as the angular coefficient of the resulting line as

$$\Delta_{\text{IMEP}}|_j \cong m|_j \cdot \Delta_{\text{MFB50}}|_j + b|_j \tag{3}$$

The parameter m is calculated cycle by cycle, based on the last N cycles IMEP and MFB50 values. Obviously, N influences the methodology dynamics: the higher its value, the slower becomes the controller in determining whether the SA must be increased or reduced. On the other hand, traditional methodologies are also based on the observation of the mean IMEP or MFB50 values over a given number of engine cycles. One advantage of the presented methodology is that the number of engine cycles necessary to establish if the combustion must be retarded or advanced is far lower to that required by the simple observation of IMEP values. This consideration is supported by Fig. 4, where the 20 cycles moving average of the IMEP and m are represented for different SA values.

The upper plot shows that the parameter m is representative of the action that the controller must take in order to maximize the IMEP; its value is systematically negative for each SA condition, meaning that the combustion must be advanced. It is also possible to notice that m absolute values tend to decrease for higher SA levels, suggesting that the combustion phasing control is close to the optimal setting. Turning to the lower plot, it is possible to appreciate how the number of engine cycles used in the moving average does not allow using IMEP as an efficient parameter to optimize combustion phasing. It is evident how different traces superimpose, and that the maximum of each trace is higher than the minimum of traces corresponding to higher SA values. For example, the trace corresponding to SA=22 deg has a minimum (cycle 212, 8.104 bars) that is far lower than the maximum for the trace corresponding to SA=20 deg (cycle 223, 8.308 bars). Though averaged over 20 engine cycles, the reported IMEP values are clearly unable to catch SA effect on IMEP. This means that it is not possible to carry out a 2 deg resolution SA optimization by using a 20 cycle basis filter on IMEP. These considerations can be repeated for the other traces represented in Fig. 4. In order to obtain an acceptable distinction of all the traces, the moving average basis should be brought to 400 engine cycles, while 20 are more than sufficient to determine the correct action on SA using the parameter m.

3 Knock Diagnosis

The previous observations do not take into consideration the knock phenomenon; the optimal combustion phasing is determined without limiting the SA to the nonknocking region.

Knocking combustions usually cause low-efficiency cycles, due to the increase in heat losses. However, it has to be reminded that,

knock being a stochastic phenomenon, a single knocking cycle is not representative of the engine running condition; a given SA could lead to a few low-efficiency cycles due to knock, but the other cycles could benefit of an increased combustion speed, leading to a better combustion phasing (i.e., higher IMEP). This explains why sometimes the highest mean IMEP values are reached under heavy knocking conditions; obviously, an automatic mapping procedure must be able to avoid dangerous combustions.

The most commonly used knock indexes (maximum amplitude of pressure oscillations (MAPO), integer derivative, third derivative, mean square value) are based on the in-cylinder pressure signal; surveys of knock indexes based on the in-cylinder pressure signal can be found in Refs. [8–12]; several indexes are compared, each one showing a different sensitivity to the knock phenomenon. These indexes are surely representative of knock effect, as it is shown in Refs. [13,14], but the relationship between their intensities and the damage risks is usually based on experience. Moreover, as it is shown in Ref. [15], knock indexes do not only depend on the phenomenon intensity, but also on external factors such as engine speed and load. Bertola et al. [16] showed that sensor type and position affect pressure oscillations measurement, and, as a consequence, knock indexes evaluation.

These considerations lead to the conclusion that it is very difficult to determine a proper threshold level for a given knock index, which can result in underperformance or damage risk. Many work in the literature associate knock-related damages to heat flux increases through the cylinder walls; Lu et al. [17] showed that for pressure oscillations above 0.5 MPa (heavy knock), the peak heat flux increases almost linearly with pressure amplitude. Other works [17–20] show that during knocking cycles high peak heat flux values can be measured, but the correlation coefficients between peak heat values and knock intensity indexes are low ($R=0.26-0.47$) for light knock, higher ($R=0.53-0.76$) for heavy knock, and strongly depend on the sensor position [17]. Grandin et al. [21–23] closely relate the peak heat flux to the increase in charge motion as a result of autoignition. They showed that for the case of the heaviest knocking condition, the peak heat flux can increase by 280% with respect to standard combustions. Ezekoye [18] made both a computational and analytical investigation of the heat transfer processes at the flame-wall interface during knock event. The analysis of the peak heat flux was conducted in three different locations: the burned gas zone, the zone of flame reactions, and the unburned zone. They concluded that the pressure transients have a moderate effect on heat transfer processes in wall locations where heat release effects are negligible (unburned zone), and modify the heat transfer rates in locations in which the flame has quenched (burned gas zone). The most important effect responsible for the magnitude of heat flux values appears to be the absolute pressure. In other words, knock indexes based on in-cylinder pressure amplitude are well related to peak heat flux. The results for different locations and timing clearly show that the peak heat flux in knocking condition is strongly increased all over the chamber. This final consideration allows extending the results on the increase in local peak heat flux all over the engine chamber.

The authors showed in previous works [24,25] that it is possible to define knock indexes based on the net Cumulative Heat Release, evaluated as follows by means of the in-cylinder pressure signal [4]:

$$\mathrm{CHR_{NET}} \int \left(\frac{\gamma}{\gamma-1} P_{\mathrm{cyl\_lp}} \frac{dV}{d\theta} + \frac{1}{\gamma-1} V \frac{dp_{\mathrm{cyl\_lp}}}{d\theta} \right) d\theta \qquad (4)$$

The net CHR for knocking cycles is lower than that of non-knocking cycles [25], due to the increase in heat losses; this information could be used for knock diagnosis, with the advantage of being directly related to the heat flux increase, i.e., to the risk of damaging the engine. In order to assess $\mathrm{CHR_{NET}}$ knock-sensitivity, its values can be related to those of other knock indexes. One of the most commonly used knock index is the MAPO, defined as

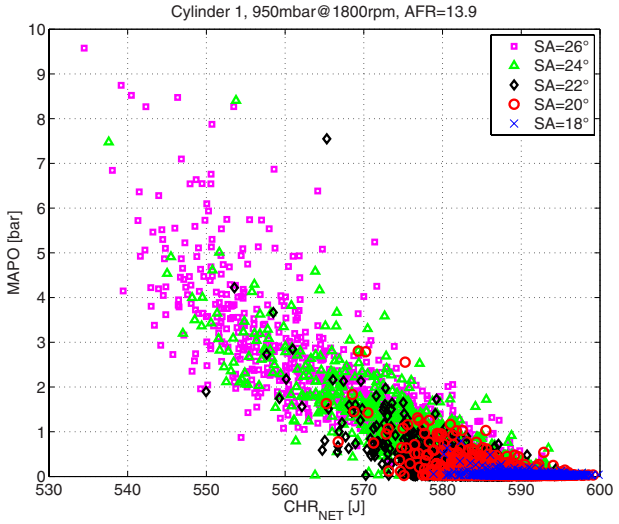

Fig. 5 MAPO versus $\mathrm{CHR_{NET}}$ distributions

$$\mathrm{MAPO} = \max\left(|p_{\mathrm{cyl\_hp}}|_{\mathrm{TDC}}^{\mathrm{TDC+70\ deg}}\right) \qquad (5)$$

Figure 5 shows that, under heavy knocking conditions, there exists a strong correlation between MAPO and $\mathrm{CHR_{NET}}$ distributions. The information that the MAPO index gives on the knock intensity is independent from the low-frequencies used to define the $\mathrm{CHR_{NET}}$ parameter. $\mathrm{CHR_{NET}}$ and MAPO actually require two different types of signal filtering: a low-pass (Butterworth, order 4, 2500 Hz) filter for the first index and a high-pass (Butterworth, order 4, 5000 Hz) for the latter. For this reason, the simultaneous use of MAPO and $\mathrm{CHR_{NET}}$ can increase the knock detection robustness. While MAPO is directly sensitive to knock, $\mathrm{CHR_{NET}}$ depends on a multitude of factors: load, speed, SA, AFR, etc: thus, as it can be noticed in Fig. 5, a knock-sensitive index based on $\mathrm{CHR_{NET}}$ should be defined using $\mathrm{CHR_{NET}}$ variations, and not its absolute value.

Statistical analyses were applied to knock detection [26–28] and are sometimes more efficient than mean values or single-value intensity evaluations in assessing the knock severity for the given running condition.

Figure 6 shows the $\mathrm{CHR_{NET}}$ probability density function plot for different SA values; in order to superimpose the distributions, the parameter $\mathrm{CHR_{NET}}$ has been normalized, dividing each value

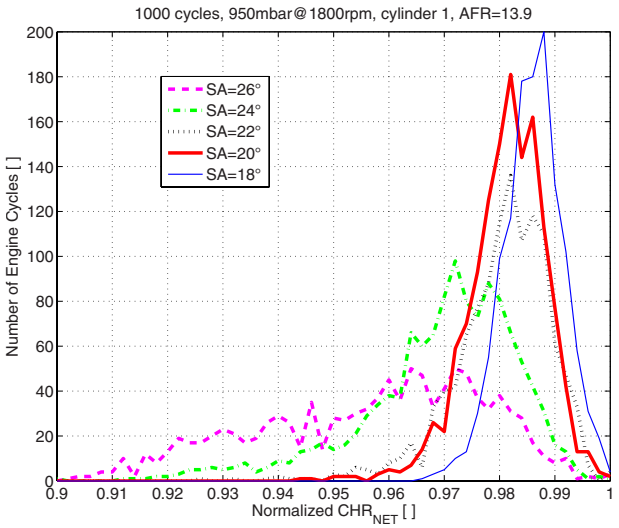

Fig. 6 $\mathrm{CHR_{NET}}$ distributions with different SA

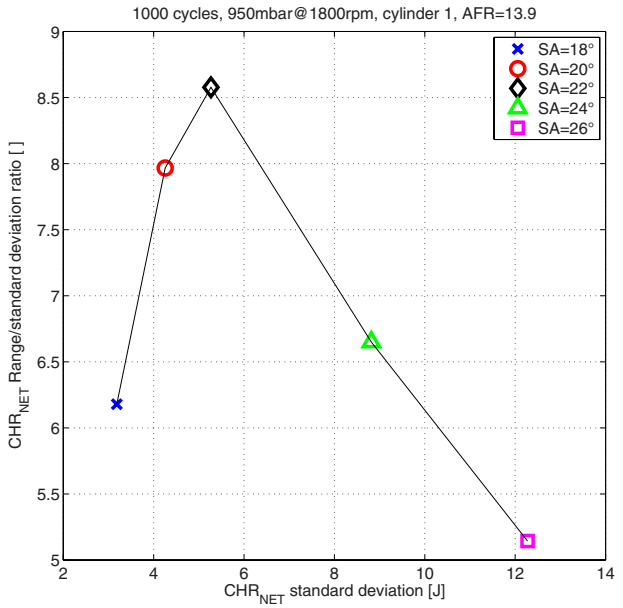

Fig. 7 Ratio between range and standard deviation for CHR_{NET}, over 1000 engine cycles

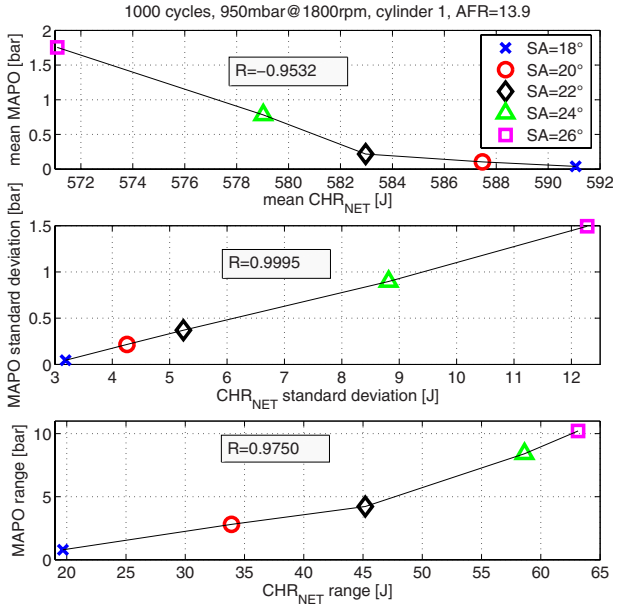

Fig. 8 Relationship between MAPO and CHR_{NET} standard deviations, range, and mean values

by the maximum of the corresponding distribution. It is possible to notice how knock affects CHR_{NET} distributions; the shape of the curve referring to SA=18 deg resembles a normal distribution, while increasing the SA, due to knock events, the shape changes, becoming asymmetric.

This behavior can be identified by means of the standard deviation or by evaluating the difference between the maximum and minimum values of CHR_{NET} for each value of SA. Even if the distributions are not exactly normal, the standard deviation gives information about the CHR_{NET} parameter dispersion for a given percentage of engine cycles (68.3% in the case of normal distribution). On the contrary, the range of CHR_{NET} is representative of a single engine cycle; the standard deviation is sensitive to the average knocking condition, while the range is representative of the heaviest knocking cycle within the sample.

A possible definition for a knock index based on CHR_{NET} can be achieved by merging the standard deviation and range information; the maximum allowable CHR_{NET} variation over the considered sample of engine cycles must be limited, both in terms of standard deviation and range.

$$\begin{aligned} \text{range}(\text{CHR}_{\text{NET}}) &< T_{\text{range\_CHR}} \\ \sigma(\text{CHR}_{\text{NET}}) &< T_{\sigma\_\text{CHR}} \end{aligned} \tag{6}$$

The two thresholds in Eq. (6) can be set, based on the engine tolerance to occasional or systematic heat flux increases. A possible solution is to define one of the two parameters, and set the other one based on the normal distribution shape. For example, $T_{\text{range\_CHR}}$ can be defined as the maximum tolerable increase in heat losses for an isolated knocking cycle. In order to enforce an equivalent limitation on CHR_{NET} standard deviation, the following consideration can be applied: For a normal distribution, the range $6\cdot\sigma$ ($\mu\pm 3\sigma$) covers the 99.7% of the samples, i.e., almost the entire range. The second limit ($T_{\sigma\text{CHR}}$) could then be equal to the first, divided by a factor of 6. This concept can be applied to the distributions shown in Fig. 6, even if they are not exactly normal; Fig. 7 shows that the actual ratio between the range and the standard deviation of the CHR_{NET} parameter varies between 5 and 8.5. It is interesting to notice that the ratio initially increases, due to sporadic knocking cycles, raising more the maximum value than the standard deviation, while, as knocking cycles become more frequent, the effect on standard deviation prevails. A similar strategy can be used for the diagnosis, based on MAPO. Threshold setting in this case is challenging, due to the index dependence on engine speed and load, sensor position, etc. The problem can be approached by comparing MAPO and CHR_{NET} distributions.

Taking into consideration the distributions corresponding to different SA values shown in the previous figures, MAPO and CHR_{NET} mean values, standard deviations, and range are all related.

This facet can be observed in Fig. 8; the reported correlation coefficients (R) suggest that MAPO and CHR_{NET} standard deviations are almost linearly related. This relationship can be used to set MAPO thresholds; it is particularly useful to take advantage of a strong linear relation because it can be estimated during nonknocking conditions, and it remains unchanged even under heavy knock. This means that the link between MAPO and CHR_{NET} standard deviations can be defined and updated in real time, without any previous information; once the engine is working in steady state, the value of the two parameters can be tracked, their linear relation coefficient estimated, and the MAPO threshold $T_{\sigma\text{MAPO}}$ can be finally determined.

As regards to the range parameter, the ratio between CHR_{NET} and MAPO values would be based on the information of a single cycle, limiting the evaluation robustness. A possible alternative approach is to accept the same ratio between the range and σ thresholds for CHR and MAPO. The threshold values can then be determined as

$$\begin{aligned} T_{\sigma\_\text{MAPO}} &= k\cdot T_{\sigma\_\text{CHR}} + q \\ T_{\text{range\_MAPO}} &= T_{\sigma\_\text{MAPO}}\cdot\frac{T_{\text{range\_CHR}}}{T_{\sigma\_\text{CHR}}} \end{aligned} \tag{7}$$

It is now possible to detect knocking events also based on MAPO index as

$$\begin{aligned} \text{range}(\text{MAPO}) &< T_{\text{range\_MAPO}} \\ \sigma(\text{MAPO}) &< T_{\sigma\_\text{MAPO}} \end{aligned} \tag{8}$$

Knock is detected when one of the conditions expressed in Eqs. (6) and (8) does not hold; in this way, both the high frequency

(MAPO) and low frequency (CHR_{NET}) in-cylinder pressure signal information content is taken into account for the detection.

4 SA Controllers

A fast and robust mapping requires the SA to be changed rapidly and coherently with IMEP variations or knock detection results. As already remarked, these operations are carried out by two independent PID controllers. The input for the first one is m, defined in Eq. (3): its value is negative when the combustion is retarded, i.e., SA must be increased. On the contrary, m tends to zero when the IMEP is near its maximum: SA must be maintained. If m is positive, it means that the combustion is too advanced, and SA must be decreased. Although m can range from $-\infty$ to $+\infty$, the values it assumes are typically in the range $[-0.1,0.1]$, as Fig. 4 suggests. This type of signal is particularly suited to feed a PID controller that will naturally tend to decrease the error, i.e., to set the optimal SA. Besides the PID gains that can be set with standard methodologies [29,30], the only parameter to set for the definition of the controller input is the number of engine cycles used to evaluate m. The final choice (10 cycles) is a tradeoff between a fast response and a stable behavior; the optimal SA must be met quickly and maintained steadily. An antiwindup saturation has been applied to the integral term of the controller; when SA is limited by knock occurrence, m may still be negative, and the integral term may grow inappropriately. The integral could also be reset when changes in operating conditions (load, speed) are detected.

As regards to SA limitations necessary to prevent knock damages, they have also been introduced by means of a PID controller; since the methodology is oriented toward mapping purposes, the correct action to take as knock happens is not just an abrupt SA reduction. The mapping operation requires a knock controller, able to maintain acceptable knock intensity levels. The controller input must be based on MAPO and CHR_{NET} standard deviations, and range, tending to zero as the allowed knock intensity is reached. This feature is guaranteed by subtracting from the threshold limit the distribution parameters (σ, range) evaluated for MAPO and CHR_{NET}

$$i_{CHR} = \min\left[\frac{T_{\sigma\_CHR} - \sigma(CHR_{NET})}{\sigma(CHR_{NET})}, \frac{T_{range\_CHR} - range(CHR_{NET})}{range(CHR_{NET})}\right] \tag{9}$$

$$i_{MAPO} = \min\left[\frac{T_{\sigma\_MAPO} - \sigma(MAPO)}{\sigma(MAPO)}, \frac{T_{range\_MAPO} - range(MAPO)}{range(MAPO)}\right]$$

To compare the inputs and decide which one must be sent to the knock controller, their values have been normalized. When the inputs are positive, the condition is nonknocking, and SA can be incremented. In the opposite hypothesis, SA must be reduced, due to knock. Only one of the two inputs will be used; as in Eq. (9), the lowest value will be chosen, meaning that the most severe of all the knock intensity evaluations is taken into consideration

$$i_{knock} = \min(i_{CHR}, i_{MAPO}) \tag{10}$$

As regards the number of engine cycles to use in the statistical analysis, it must be large enough to be significant of the knock behavior for the given condition, but still small enough to perform a fast mapping procedure. The results reported in the following are based on a 200 cycle sample.

Figure 9 shows the controller input values in tests carried out with the controller deactivated and constant SA. It can be seen that, while the value of i_{knock} is always positive for SA=18 deg, it sometimes becomes negative for SA=20 deg, marking the beginning of knock phenomena. The controller input tends to be always negative for higher SA levels; under these conditions, the controller will certainly tend to reduce SA.

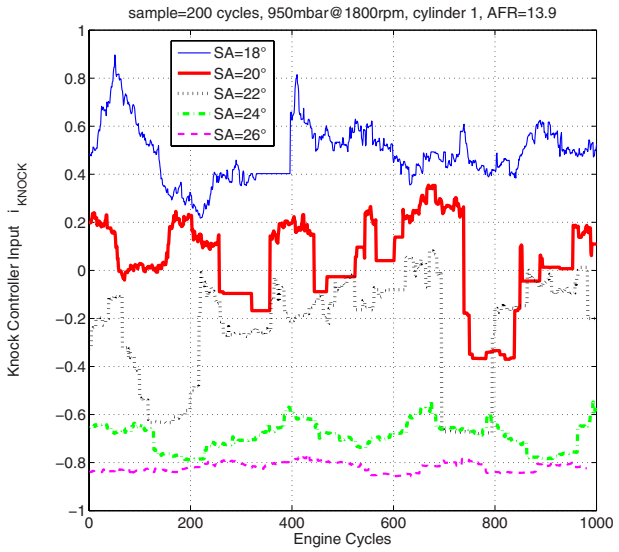

Fig. 9 Knock controller input

5 Results

The controller calibration and the analysis of the control system behavior has been carried out offline. For a given operating condition defined by engine speed and load, tests have been run with constant SA; each test consists of 1000 engine cycles, thus, it is able to represent the combustion characteristic for a given control setting, both from mean values and stochastic distribution points of view. In-cylinder pressure signals have been sampled during the tests, and processed offline, in order to evaluate indicating parameters such as IMEP, CHR, MFB50, and knock indexes (MAPO). All the cycle-based data have been assembled into combustion matrices, with each column corresponding to a different SA value, and each row representing the indicating or knock parameter cycle-by-cycle evolution. The matrices can be used to copy the engine behavior under the influence of a feedback controller regulating the SA value. The number of columns of the matrices depends on the range and resolution of SA variations applied during the tests. The SA controllers outputs could require SA values placed between two subsequent brake points of the tests grid; indicating and knock parameters in this case are obtained by means of an interpolation between the values found for the given row, in the previous and succeeding columns. Finally, in order to eliminate any dependence on the indicating and knock parameters cycle-to-cycle pattern found in the sampled data, the order of the combustion matrices elements is randomized column by column, each time a simulation is launched.

Figure 10 shows the action of the controller managing the SA for optimal IMEP; in this case, the knock controller is deactivated. It can be seen that SA is rapidly increased until it reaches the value that maximizes IMEP. After that, it is maintained steady; the oscillations and the controller response can be tuned by means of the PID control constants, or, as it is shown in the figure, by filtering the controller outputs with a moving average filter. It can be seen that after 1000 cycles, the oscillation band is restricted to ± 0.2 deg; obviously, a smaller band can be obtained by changing the controller parameters. It can also be noticed that in less than 400 cycles, the controller brings SA in the range of ± 1 deg with respect to the optimal value. The real advantage of the methodology, however, is to concentrate the SA sweep in a single test. The performance could be improved, but it has to be reminded that the IMEP optimizer has to cooperate with the knock controller that needs a larger number of engine cycles in order to evaluate knock intensity.

Figure 11 shows the superimposition of ten simulations, each one carried out with different random cycle sequences, confirming

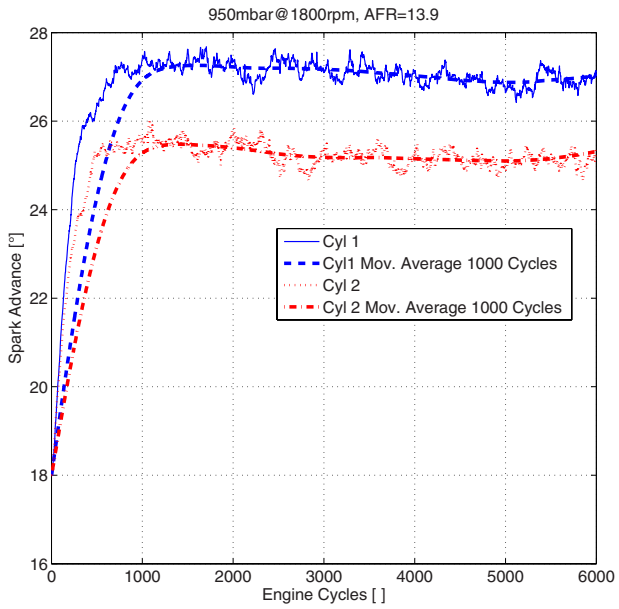

Fig. 10 SA control for optimal IMEP

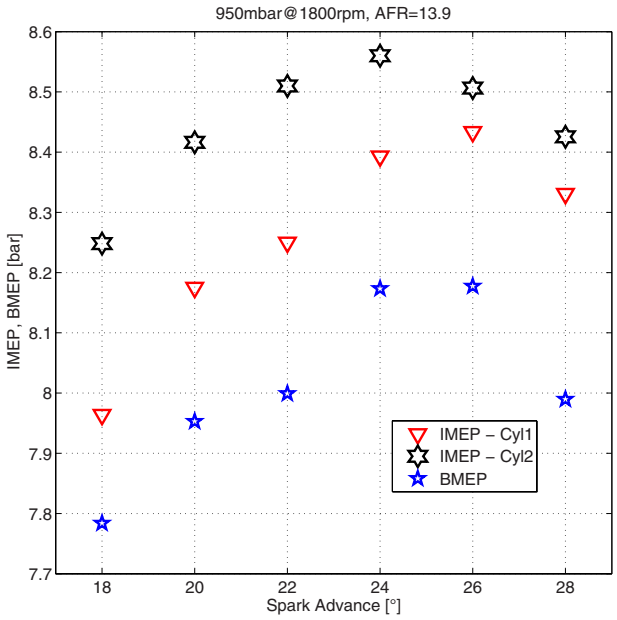

Fig. 12 IMEP and BMEP mean values

that the results do not depend on the pattern of engine cycles used for the simulation. The oscillation bandwidth is once again ±0.2°.

The controller actually leads to the maximum IMEP, as can be seen in Fig. 12, where the IMEP for cylinders 1 and 2, and BMEP mean values, are reported.

The knock controller has to stop the IMEP optimizer as knock is detected, limiting the SA value to the tolerable knock threshold. Figure 13 shows how the two controllers modify the SA during a simulated test; first, the IMEP optimizer requires a rapid increase in SA, due to the high error input. Then, after knock is detected, the knock controller decreases the SA until it is smoothed to a knock-safe level. The process can be considered terminated after 3000 engine cycles, when the SA value oscillates in the range of ±0.2° with respect to the average.

The proposed approach proves to be efficient and precise in determining optimal SA values, taking into account IMEP optimization and knock diagnosis. The methodology will be implemented in a real time combustion control system described in Ref. [31] that is able to analyze the in-cylinder pressure signal, determining in real time, cycle by cycle, indicated and knock parameters. Further work will be devoted to the controllers' improvement with an extension to transient conditions that could lead to an on-board application.

6 Conclusions

The paper presents a SA mapping approach based on the statistical analysis of in-cylinder pressure based indexes; the objectives are to maximize IMEP and to limit knock to acceptable levels.

The combustion event is described by means of the MFB50 parameter, and the observation of the trend IMEP-MFB50 allows defining a suitable parameter to use as input for the SA controller in charge of the IMEP optimization.

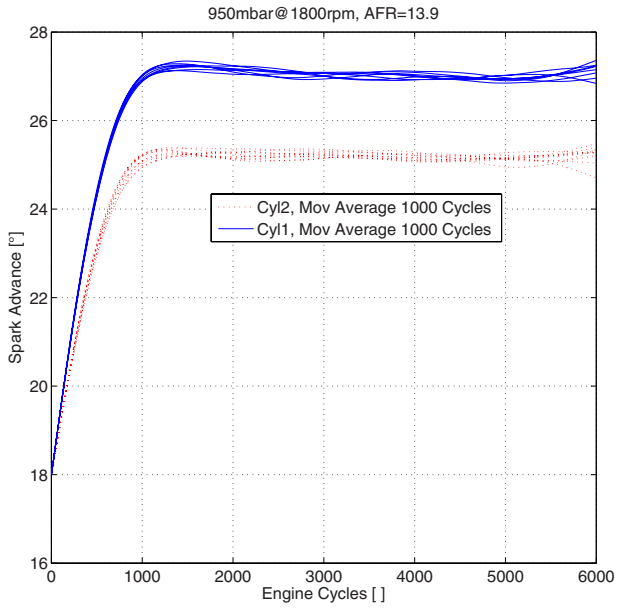

Fig. 11 Simulations superimposition

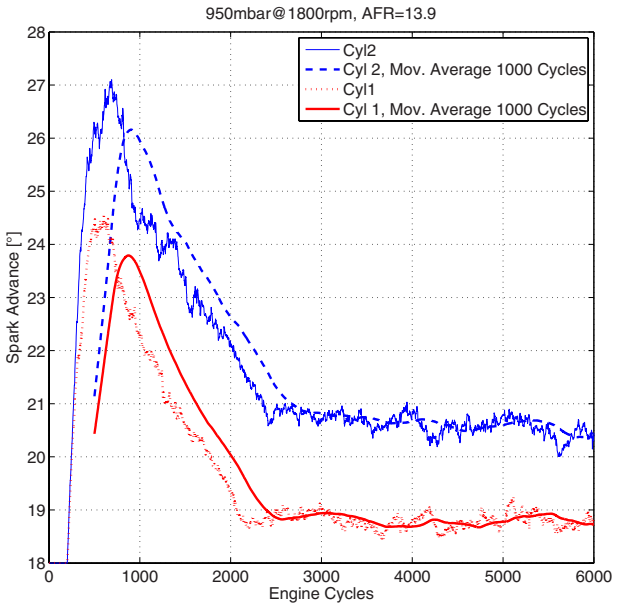

Fig. 13 SA control with both the controllers activated

Knock diagnosis is carried out by comparing the distributions of two knock-sensitive parameters; CHR_{NET} is based on the low frequency content of the in-cylinder pressure signal, while MAPO is based on the high frequency content. Both sporadic and systematic knock effects must be taken into account, thus, standard deviation and range of the two parameters within a given buffer of engine cycles are considered as knock-sensitive indexes. Thresholds are set for CHR_{NET}, and the relationships between the distributions can be used to set thresholds for MAPO. The distance from the thresholds are then used as inputs for the SA knock limiter controller.

The methodology has been applied offline, showing that the optimal SA can be determined within 3000 engine cycles.

Nomenclature

a = Wiebe function parameter
AFR = air to fuel ratio
b_j = y-intercept for the line interpolating $\Delta_{MFB50}|_j$ versus $\Delta_{IMEP}|_j$ distribution
BSFC = brake specific fuel consumption
c = Offset for the relationship between CHR_{NET} and MAPO standard deviations
CHR_{NET} = net cumulative heat release
δ_{MFB50}, δ_{IMEP} = MFB50 and IMEP cycle-to-cycle variations
Δ_{MFB50}, Δ_{IMEP} = vectors containing the last N values of δ_{MFB50} and δ_{IMEP}
ECU = electronic control unit
i_{CHR} = input of the knock controller based on CHR_{NET}
i_{MAPO} = input of the knock controller based on MAPO
IMEP = indicated mean effective pressure
K = angular coefficient of the line interpolating T_{σ_MAPO} versus T_{σ_CHR} distribution
γ = specific heat ratio
m_j = angular coefficient of the line interpolating $\Delta_{MFB50}|_j$ versus $\Delta_{IMEP}|_j$ distribution
m_W = Wiebe function parameter
MAMFB = maximum acceleration of mass fraction burned
MAPO = maximum amplitude of pressure oscillations
MBT = maximum brake torque
MFB50 = angular position corresponding to: fuel mass fraction burned = 50%
N = number of engine cycles in the buffer
P_{cyl_lp} = low-pass filtered cylinder pressure (Butterworth, 3 kHz)
P_{cyl_hp} = high-pass filtered cylinder pressure (Butterworth, 5 kHz)
PFI = port fuel injection
PID = proportional-integer-derivative (controller)
R = linear correlation coefficient (Bravais–Pearson)
ROHR = rate of heat release
q = y-intercept for the line interpolating T_{σ_MAPO} versus T_{σ_CHR} distribution
SI = spark ignition
SA = spark advance
T_{range_CHR} = maximum allowable CHR_{NET} range
T_{range_MAPO} = maximum allowable MAPO range
T_{σ_CHR} = maximum allowable CHR_{NET} standard deviation
T_{σ_MAPO} = maximum allowable MAPO standard deviation
TDC = top dead center
V = cylinder volume
V_d = cylinder displacement
x_b = mass fraction burned
$\Delta\theta$ = combustion duration
σ = standard deviation
θ = crankshaft angle
θ_{SOC} = angle corresponding to the start of combustion

References

[1] Viebe, I. I., 1956, "Semi-Empirical Expression for Combustion Rate in Engines," *Proceedings of the Conference on Piston Engines*, USSR Academy of Sciences, Moscow, pp. 185–191.
[2] Jante, A., 1960, "The Wiebe Combustion Law (Das Wiebe-Brenngesetz, ein Forschritt in der Thermodynamik der Kreisprozesse von Verbrennungsmotoren)," Kraftfharzeugtechnik, **9**, pp. 340–346.
[3] Roelle, M. J., Shaver, G. M., and Gerdes, J. C., 2004, "Tackling the Transition: A Multi-Mode Combustion Model of SI and Hcci for Mode Transition Control," *Proceedings of the IMECE 04, 2004 International Mechanical Engineering Conference and Exposition*.
[4] Heywood, J. B., 1988, *Internal Combustion Engine Fundamentals*, McGraw-Hill, New York.
[5] Ponti, F., Corti, E., Serra, G., and De Cesare, M., 2007, "Common Rail Multi-Jet Diesel Combustion Engine Model Development for Control Purposes," *Proceedings of the SAE World Congress*, Paper No. 2007-01-0383.
[6] Patterson, G. J., 2008, "A Technique for Processing Cylinder Pressure and Test Bed Data Sets for Engine Speed-Sweep Tests to Allow Reduced Testing Time With Enhanced Interpretation of Results," *Proceedings of the SAE Motorsports 2008 Conference*, Paper No. SAE2008-01-3006.
[7] Haskara, I., Zhu, G. G., Daniel, C. F., and Winkelman, J., 2004, "On Combustion Invariance for MBT Timing Estimation and Control," ASME Paper No. ICEF2004-835.
[8] Worret, R., Bernhardt, S., Schwarz, F., and Spicher, U., 2002, "Application of Different Cylinder Pressure Based Knock Detection Methods in Spark Ignition Engines," *Proceedings of the SAE World Congress*, Paper No. 2002-01-1668.
[9] Brecq, G., Bellettre, J., and Tazerout, M., 2001, "Experimental Determination of Knock in Gas SI Engines," *Proceedings of the SAE World Congress*, Paper No. 2001-28-0022.
[10] Millo, F., and Ferraro, C. V., 1998, "Knock in S.I. Engines: A Comparison Between Different Techniques for Detection and Control," *Proceedings of the SAE World Congress*, p. 982477.
[11] Brecq, G., Bellettre, J., and Tazerout, M., 2003, "A New Indicator for Knock Detection in Gas SI Engines," Int. J. Therm. Sci., **42**, pp. 523–532.
[12] Xiaofeng, G., Stone, R., Hudson, C., and Bradbury, I., 1993, "The Detection and Quantification of Knock in Spark Ignition Engines," *Proceedings of the SAE World Congress*, p. 932759.
[13] Nates, R. J., and Yates, A. D. B., 1994, "Knock Damage Mechanisms in Spark-Ignition Engines," *Proceedings of the SAE World Congress*, p. 942064.
[14] Fitton, J., and Nates, R., 1996, "Knock Erosion in Spark-Ignition Engines," *Proceedings of the SAE World Congress*, p. 962102.
[15] Minelli, G., Corti, E., Moro, D., and Solieri, L., 2006, "Knock Indexes Normalization Methodologies," *Proceedings of the SAE World Congress*, Paper No. 2006-01-2998.
[16] Bertola, A., Stadler, J., Walter, T., Wolfer, P., Gossweiler, C., and Rothe, M., 2006, "Pressure Indication During Knocking Conditions," *Proceedings of the Seventh International AVL Symposium on Internal Combustion Diagnostics*.
[17] Lu, J.-h., Ezekoye, D., Iiama, A., Greif, R., and Saweye, R. F., 1989, "Effect of Knock on Time-Resolved Engine Heat Transfer," *Proceedings of the SAE World Congress*, p. 890158.
[18] Ezekoye, O. A., 1995, "Heat Transfer Modeling During Knock and Flame Quenching in an Engine Chamber," *Proceedings of the 26th Symposium on Combustion*, Combustion Institute, pp. 2661–2668.
[19] Syrimis, M., Shigahara, K., and Assanis, D. N., 1996, "Correlation Between Knock Intensity and Heat Transfer Under Light and Heavy Knocking Conditions in a Spark Ignition Engine," *Proceedings of the SAE World Congress*, p. 960495.
[20] Syrimis, M., Shigahara, K., and Assanis, D. N., 1997, "Piston Heat Transfer Measurements Under Varying Knock Intensity in a Spark-Ignition Engine," *Proceedings of the SAE World Congress*, p. 971667.
[21] Grandin, B., Denbratt, I., Bood, J., Brackmann, C., and Bengtsson, P. E., 2000, "The Effect of Knock on the Heat Transfer in an S.I. Engine: Thermal Boundary Layer Investigation Using CARS Temperature Measurements and Heat Flux Measurements," *Proceedings of the SAE World Congress*, Paper No. 2000-01-2831.
[22] Grandin, B., Denbratt, I., Bood, J., Brackmann, C., Bengtsson, P. E., Gogan, A., Mauss, F., and Sunden, B., 2002, "The Effect of Knock on Heat Transfer in S.I. Engines," *Proceedings of the SAE World Congress*, Paper No. 2002-01-0238.
[23] Grandin, B., Denbratt, I., Bood, J., Brackmann, C., Bengtsson, P. E., Gogan, A., Mauss, F., and Sunden, B., 2002, "Heat Release in the End-Gas Prior to Knock in Lean, Rich and Stoichiometric Mixtures With and Without EGR," *Proceedings of the SAE World Congress*, Paper No. 2002-01-0239.
[24] Cavina, N., Corti, E., and Solieri, L., 2006, "A Heat Flux Damages-Related Index," ASME Paper No. ICES2006-1425.
[25] Corti, E., and Forte, C., "Statistical Analysis of Indicating Parameters for Knock detection Purposes," *Proceedings of the SAE World Congress*, Paper No. 2009-01-0237.

[26] Campbell, J., and Lovell, W. G., 1938, "Application of Statistical Concepts to the Knock-Rating Problem," SAE Technical Paper No. 380169.
[27] Wu, G., 2007, "A Real Time Statistical Method for Engine Knock Detection," *Proceedings of the SAE World Congress*, Paper No. 2007-01-1507.
[28] Zhu, G. G., Haskara, I., and Winkelman, J. R., 2005, "Stochastic Limit Control and Its Application to Knock Limit Control Using Ionization Feedback," *Proceedings of the SAE World Congress*, Paper No. 2005-01-0018.
[29] Franklin, G., Powell, J. D., and Emani-Naeini, A., 2006, *Feedback Control of Dynamics Systems*, Prentice-Hall, Englewood Cliffs, NJ.
[30] Goodwin, G., Graebe, S. F., Salgado, M. E., 2001, *Control System Design*, Prentice-Hall, Englewood Cliffs, NJ.
[31] Corti, E., Moro, D., and Solieri, L., 2007, "Real-Time Evaluation of IMEP and ROHR-Related Parameters," *Proceedings of the SAE ICE 2007 International Conference*, Paper No. SAE2007-24-0068.